BMP4 Increases Canonical Transient Receptor Potential Protein Expression by Activating p38 MAPK and ERK1/2 Signaling Pathways in Pulmonary Arterial Smooth Muscle Cells

Xiaoyan Li[1,2*], Wenju Lu[1,2*], Xin Fu[1*], Yi Zhang[1,2], Kai Yang[1,2], Nanshan Zhong[1], Pixin Ran[1], and Jian Wang[1,2]

[1]State Key Laboratory of Respiratory Diseases, Guangzhou Institute of Respiratory Disease, First Affiliated Hospital of Guangzhou Medical University, Guangzhou, Guangdong, People's Republic of China; and [2]Division of Pulmonary and Critical Care Medicine, Johns Hopkins Medical Institutions, Baltimore, Maryland

Abnormal bone morphogenetic protein (BMP) signaling has been implicated in the pathogenesis of pulmonary hypertension. We previously found that BMP4 elevated basal intracellular Ca^{2+} ($[Ca^{2+}]_i$) concentrations in distal pulmonary arterial smooth muscle cells (PASMCs), attributable in large part to enhanced store-operated Ca^{2+} entry through store-operated Ca^{2+} channels (SOCCs). Moreover, BMP4 up-regulated the expression of canonical transient receptor potential (TRPC) proteins thought to compose SOCCs. The present study investigated the signaling pathways through which BMP4 regulates TRPC expression and basal $[Ca^{2+}]_i$ in distal PASMCs. Real-time quantitative PCR was used for the measurement of mRNA, Western blotting was used for the measurement of protein, and fluorescent microscopic for $[Ca^{2+}]_i$ was used to determine the involvement of p38 and extracellular regulated kinase (ERK)–1/2 mitogen-activated protein kinase (MAPK) signaling in BMP4–induced TRPC expression and the elevation of $[Ca^{2+}]_i$ in PASMCs. We found that the treatment of BMP4 led to the activation of both p38 MAPK and ERK1/2 in rat distal PASMCs. The induction of TRPC1, TRPC4, and TRPC6 expression, and the increases of $[Ca^{2+}]_i$ caused by BMP4 in distal PASMCs, were inhibited by treatment with either SB203580 (10 μM), the selective inhibitor for p38 activation, or the specific p38 small interfering RNA (siRNA). Similarly, those responses induced by BMP4 were also abolished by treatment with PD98059 (5 μM), the selective inhibitor of ERK1/2, or by the knockdown of ERK1/2 using its specific siRNA. These results indicate that BMP4 participates in the regulation of Ca^{2+} signaling in PASMCs by modulating TRPC channel expression via activating p38 and ERK1/2 MAPK pathways.

Keywords: BMP4; intracellular Ca^{2+} concentration; TRPC; p38 MAPK; ERK1/2

(*Received in original form August 24, 2011 and in final form February 13, 2013*)

* These authors contributed equally to this article.

This work was supported by National Institutes of Health Research Grant R01HL093020 (J.W.), National Natural Science Foundation of China grants 81070043, 81071917, 81173112, 81170052, 81200037, and 81220108001, Chinese Central Government Key Research Projects of the 973 grant 2009CB522107, Changjiang Scholars and Innovative Research Team University Grant IRT0961, Guangdong Department of Science and Technology of China grants 2009B050700041 and 2010B031600301, Guangdong Province Universities and Colleges Pearl River Scholar Funded Scheme (2008), Guangdong Department of Education Research Grant CXZD1025, Guangdong Natural Science Foundation Team Grant 1035101200300000, and Guangzhou Department of Education Yangcheng Scholarships 10A058S and 12A001S. X.L. was an exchange doctoral candidate student supported by the Chinese Scholarship Council (2008).

Correspondence and requests for reprints should be addressed to Jian Wang, Ph.D., State Key Laboratory of Respiratory Diseases, 1st Affiliated Hospital of Guangzhou Medical University, Guangzhou, Guangdong, China. E-mail: jwang31@jhmi.edu

This article has an online supplement, which is accessible from this issue's table of contents at www.atsjournals.org

Am J Respir Cell Mol Biol Vol 49, Iss. 2, pp 212–220, Aug 2013

Originally Published in Press as DOI: 10.1165/rcmb.2012-0051OC on March 20, 2013
Internet address: www.atsjournals.org

Pulmonary arterial hypertension (PAH) is a lethal disease characterized by elevated pressure and vascular wall remodeling in pulmonary arteries (PAs). Although many years of extensive investigation have advanced our understanding of PAH, the mechanisms underlying its pathogenic changes remain elusive. Studies using animal models of chronic hypoxic pulmonary hypertension (CHPH) have revealed that the basal intracellular Ca^{2+} ($[Ca^{2+}]_i$) concentration in pulmonary arterial smooth muscle cells (PASMCs) is elevated, and this elevation functions as a key element in the pathogenesis of PAH by facilitating not only vasoconstriction but also the growth and migration of cells (1–3). However, the detailed molecular mechanisms underlying this elevated change of $[Ca^{2+}]_i$ in PASMCs are largely unclear.

In vascular smooth muscle cells, the rise of $[Ca^{2+}]_i$ can occur through a depletion of Ca^{2+} stores, increased Ca^{2+} influx from an extracellular source via Ca^{2+} channels, or reduced Ca^{2+} efflux via Ca^{2+}-ATPases and the Na^+/Ca^{2+} exchanger on the plasma membrane (3, 4). In PASMCs during CHPH, the increases in basal $[Ca^{2+}]_i$ and the maintenance of cell contraction appear attributable to the activation of Ca^{2+} influx through pathways other than voltage-dependent Ca^{2+} channels (VDCCs), because the removal of extracellular Ca^{2+}, but not of VDCC blockers, decreased $[Ca^{2+}]_i$ in PASMCs during chronic hypoxia, and relaxed arteries in chronically hypoxic rats (5). Store-operated calcium channels (SOCCs) are believed to be composed of members of transient receptor potential canonical (TRPC) family, which assemble as either homotetramer or heterotetramer channels and mediate store-operated calcium entry (SOCE) (6). We recently demonstrated the predominant expression of TRPC1, TRPC4, and TRPC6, and the presence of SOCE in PASMCs (7). Exposure to chronic hypoxia enhanced the expressions of TRPC1, TRPC6, and SOCE in rat distal PASMCs (1, 2). Using a specific small interfering (si)RNA individually targeted to TRPC1 and TRPC6, we found they both contributed to the hypoxic enhancement of SOCE and the maintenance of elevated basal $[Ca^{2+}]_i$ in PASMCs (8). These studies provided fundamental information indicating that the elevation of basal $[Ca^{2+}]_i$ in PASMCs during chronic hypoxia are in large part caused by enhanced SOCE via the up-regulation of TRPC proteins.

Bone morphogenetic protein (BMP) family members comprise multifunctional cytokines that play crucial roles during embryonic development, organogenesis, and adult tissue remodeling by regulating cell proliferation, growth, differentiation, and apoptosis (9). BMP4, which is essential for lung development, was recently found to be up-regulated by hypoxia in murine lung tissue, driving the proliferation and migration of PASMCs, and thus promoting pulmonary arterial remodeling during the development of CHPH (10–12). The signaling of BMP4 involves binding to its Type I and Type II serine/threonine kinase receptors and the subsequent activation of Smad-dependent and Smad-independent pathways,

resulting in the regulation of a plethora of genes related to cell function (13). The Smad pathway is the canonical pathway thought to mediate the antiproliferative or proapoptotic effects of various BMP ligands. Accumulating evidence indicates that the proliferative effects of BMP4 on PASMCs are transmitted through Smad-independent pathways, including extracellular signal–regulated kinase–1/2 (ERK1/2) and p38 mitogen-activated protein kinase (p38 MAPK) signaling (14–16).

We previously demonstrated that BMP4 up-regulated TRPC1, TRPC4, and TRPC6 expression, leading to enhanced SOCE and elevated basal $[Ca^{2+}]_i$ in distal PASMCs (3). In this study, we further examined whether these effects of BMP4 are regulated through p38 MAPK–mediated and/or ERK1/2-mediated pathways.

MATERIALS AND METHODS

Rat Distal PASMC Culture

All procedures during our animal experiments were approved by the Animal Care and Use Committees at the Johns Hopkins University School of Medicine and the First Affiliated Hospital of Guangzhou Medical University. Adult male Wistar rats (300–500 g) were used to isolate distal pulmonary arteries (PAs, >4 generations) and grow PASMCs, as previously described (3, 6). Briefly, the endothelium-denuded pulmonary artery (PA) tissue was digested. Cells were plated onto 35-mm dishes or six-well plastic dishes, and cultured for 3 to 4 days in smooth muscle growth medium–2 (SmGM-2; Clonetics, Walkersville, MD) containing 5% serum. The cellular purity of PASMCs in all experiments was assessed to be greater than 95% according to α-actin immunostaining and cell counting under fluorescent microscopy.

BMP4, MAPK Inhibitors, and siRNA Treatments

After 24 hours of quiescence in smooth muscle basic medium (SmBM; Clonetics) containing 0.3% serum, PASMCs were treated with 50 ng/ml recombinant human BMP4 (R&D Systems, Minneapolis, MN) or an equivalent volume of its vehicle (4 mM HCl containing 0.1% BSA) for up to 60 hours. In inhibitor studies, PASMCs were pretreated with p38 MAPK inhibitor SB203580 (10 μM; Cell Signaling Technology, Danvers, MA), ERK1/2 inhibitor PD98059 (5 μM; Cell Signaling Technology), or their dissolvent dimethyl sulfoxide (DMSO) for 30 minutes. The treatment of PASMCs with siRNA was modified from a previous procedure (17). Briefly, cells were transfected with 50 nM siRNA for 24 hours, using GeneSilencer (Genlantis, San Diego, CA) before treatments with BMP4. ERK1/2 and p38 MAPK siRNA were designed and synthesized by GenePharma, Ltd. (Shanghai, China). The siRNA sequences are included in Table 1. Nontargeting siRNA (Dharmacon, Lafayette, CO) was used for control purposes.

Measurement of Intracellular Ca^{2+} Concentrations

The basal $[Ca^{2+}]_i$ concentration in PASMCs was measured using Fura-2 dye and fluorescent microscopy, as we described elsewhere (6, 29). Briefly, cells were loaded with 7.5 μM Fura-2 acetoxymethyl (AM) (Invitrogen, Carlsbad, CA) for 60 minutes at 37°C in an atmosphere of 5% CO_2–95% air. The loaded coverslips with PASMCs were mounted in a closed polycarbonate chamber, clamped in a heated aluminum platform (PH-2; Warner Instruments, Hamden, CT) on the stage of a Nikon TSE100 Ellipse inverted microscope (Nikon, Melville, NY), and perfused at 0.5–1 ml/minute with Krebs Ringer bicarbonate (KRB) solution, which contained 118 mM NaCl, 4.7 mM KCl, 2.5 mM $CaCl_2$, 0.57 mM $MgSO_4$, 1.18 mM KH_2PO_4, 25 mM $NaHCO_3$, and 10 mM glucose. The KRB solution was equilibrated with 5% CO_2 and 16% O_2 concentrations at 38°C in heated reservoirs, and led via stainless steel tubing and a manifold to an inline heat exchanger (SF-28; Warner Instruments), which rewarmed the perfusate just before entering the cell chamber. Chamber temperature was maintained at 37°C with an inline heat exchanger and dual-channel heater controller (SF-28 and TC-344B; Warner Instruments). After perfusing the chamber for 10 minutes to remove extracellular dye, we measured Fura-2 fluorescence emitted at 510 nm after excitation at 340 and 380 nm at 12- to 30-second intervals in 15 to 30 cells using a xenon arc lamp, interference filters, and an electronic shutter, and focused on PASMCs visualized with a ×20 fluorescence objective (Super Fluor 20; Nikon, Torrance, CA). An electronic shutter (Vincent Associates, Rochester, NY) was used to minimize photobleaching. Data were collected online with InCyte software (Intracellular Imaging, Cincinnati, OH).

RNA Extraction and Quantitative Real-Time PCR

Total RNA was extracted from rat distal PASMCs, using an RNeasy Mini Kit (Qiagen, Valencia, CA) according to the manufacturer's instructions. DNA from each RNA sample was removed by TURBO DNA-free DNase I (Applied Biosystems, Grand Island, NY). Reverse transcription was performed using StrataScript first-strand synthesis system (Bio-Rad Laboratories, Carlsbad, CA). Synthesized complementary DNA was amplified by a standard PCR protocol, using the iQ SYBR Green Supermix (Bio-Rad Laboratories). The primer sequences for TRPC1, TRPC4, TRPC6, ERK1/2, p38, and cyclophilin B were designed using the online program Primer3 (www-genome.wi.mit.edu/cgi-bin/primer/primer3_www.cgi), and are listed in Table 1. Cyclophilin B was used as an internal control for DNA loading during PCR. The PCR cycling conditions involved 30 seconds at 95°C for two cycles, followed by 45 cycles of 15 seconds at 94°C, 20 seconds at 57.5°C, and 2 seconds at 72°C. The specificity of

TABLE 1. REAL-TIME QUANTITATIVE PCR PRIMERS AND siRNA SEQUENCES

Gene	Accession Number	Oligo DNA Sequence	Product Size (bp)	Location in Sequence
TRPC1 primers	NM_053558	Left: 5′-AGCCTCTTGACAAACGAGGA-3′ Right: 5′-ACCTGACATCTGTCCGAACC-3′	146	797–942
TRPC4 primers	NM_080396	Left: 5′-GACACGGAGTTCCAGAGAGC-3′ Right: 5′-GTTGGGCTGAGCAACAAACT-3′	142	777–918
TRPC6 primers	NM_053559	Left: 5′-TACTGGTGTGCTCCTTGCAG-3′ Right: 5′-GAGCTTGGTGCCTTCAAATC-3′	141	1267–1407
ERK1 primers	NM_017347	Left: 5′-CTG GCTTTCTGACCGAGTATGTGG-3′ Right: 5′-CAGCTCCTTCAGCCGCTCC-3′	498	598–1095
ERK2 primers	NM_053842	Left: 5′-TGAGCACCAGACCTACTGTCAGAG-3′ Right: 5′- GGTTGGAAGGCTTGAGGTCAC-3′	265	172–436
Cyclophilin B primers	NM_022536	Left: 5′-GGACGAGTGACCTTTGGACT-3′ Right: 5′-TGACACGATGGAACTTGCTG-3′	118	170–287
ERK1 siRNA	NM_017347	Sense: 5′-GCUACACCAAAUCCAUUGATT-3′ Antisense: 5′-UCAAUGGAUUUGGUGUAGCTT-3′		689–707
ERK2 siRNA	NM_053842	Sense: 5′-CCAGGAUACAGAUCUUAAATT-3′ Antisense: 5′-UUUAAGAUCUGUAUCCUGGTT-3′		1231–1249
p38 siRNA	NM_031020	Sense: 5′- GACCUCCUUAUAGACGAAUTT-3′ Antisense:5′-AUUCGUCUAUAAGGAGGUCTT-3′		1294–1312

Definition of abbreviations: bp, base pairs; ERK, extracellular signal–regulated kinase; TRPC, transient receptor potential.

amplification was confirmed by running the melting curve after each PCR run. The cycle of threshold for samples and the real-time PCR efficiency of each gene were generated by iCycler software (Bio-Rad Laboratories). The copy numbers of target gene mRNAs were calculated using the method of Pfaffl (18).

Western Blot Analysis

Cells were lysed with TPER lysis buffer (Pierce, Rockford, IL) supplemented with proteinase inhibitors (Sigma Chemical Co., St. Louis, MO). Cell lysate proteins were separated by 10% SDS-PAGE and then transferred to polyvinylidene fluoride membrane (pore size of 0.45 μM; Bio-Rad Laboratories). The proteins on membranes were blotted with TRPC1 (Sigma Chemical Co.), TRPC4 (Santa Cruz Biotechnology, Santa Cruz, CA), TRPC6 (Alomone Laboratories, Jerusalem, Israel), and phospho-ERK1/2 or phospho–p38 MAPK (Cell Signaling Technology, Inc.) antibodies. Membranes were also blotted with ERK1/2 (Cell Signaling Technology, Inc.), p38 MAPK (Cell Signaling Technology, Inc.), or α-actin (Sigma Chemical Co.) antibodies to serve as controls for equal protein loading. The bound antibodies were probed with peroxidase-labeled anti-rabbit or anti-mouse IgG (KPL, Inc., Gaithersburg, MD), and the signals were developed by enhanced chemiluminescence reagents (GE Healthcare, Piscataway, NJ).

Materials and Drugs

Unless otherwise specified, all reagents were obtained from Sigma-Aldrich (St. Louis, MO). The recombinant human BMP4 stock solutions at 50 μg/ml were produced in 4 mM HCl containing 0.1% BSA. Stock solutions of SB203580 (10 mM) and PD98059 (5 mM) were produced in DMSO. Fura-2 AM was prepared on the day of the experiment as a 2.5-mM stock solution in DMSO containing 20% pluronic F-127 (Invitrogen).

Statistical Analysis

Data in bar graphs are expressed as means ± SEMs, and *n* indicates the number of experiments performed, which is the same as the number of animals providing PASMCs. When Fura-2 fluorescence was measured for assessing $[Ca^{2+}]_i$, the number of cells in each experiment ranged from 25 to 40, as indicated in figure legends. Statistics were analyzed using ANOVA and the Student *t* test. If significant *F* ratios were obtained with ANOVA, a pairwise comparison of means was performed using *t* tests. Differences in comparisons at $P < 0.05$ were considered significant.

RESULTS

Treatment of BMP4 Induced the Activation of p38 and ERK1/2 in Rat Distal PASMCs

BMP4 treatment led to p38 and ERK1/2 phosphorylation in human PASMCs (14). To verify whether similar responses also happened in rat cells, we treated rat distal PASMCs with 50 ng/ml BMP4 for various amount of time from 15 minutes (0.25 hour) up to 60 hours, and observed the activation of p38 and ERK1/2 MAPKs by Western blotting. As shown in Figures 1A and 1B, p38 was activated by BMP4 early, as of 0.25 hour. The activation was sustained for up to 60 hours. In contrast, the activation of ERK1/2 by BMP4 began at 0.25 hour, followed by reduced concentrations from 0.5 to 4 hours, returning to baseline when observed at the 8-hour and 60-hour time points (Figures 1C and 1D). These results indicate that BMP4 challenge does cause p38 and ERK1/2 activation in rat distal PASMCs.

Pretreatment with p38 and ERK1/2 Inhibitors Prevented Their Activation by BMP4

To examine whether p38 and ERK1/2 signaling were involved in BMP4–induced TRPC expression in rat distal PASMCs, we first examined the efficacy and specificity of their inhibitors on the BMP4-induced activation of p38 and ERK1/2. Cells were pretreated with the p38 inhibitor SB203580 or the ERK1/2

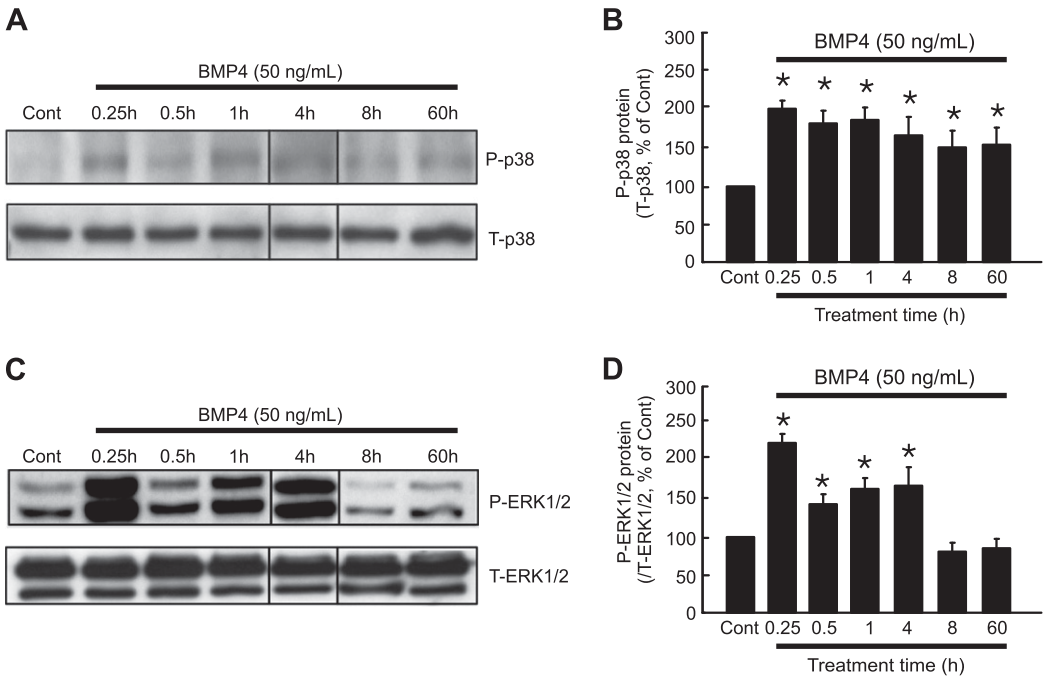

Figure 1. Bone morphogenetic protein (BMP)–4 increased p38 mitogen-activated protein kinase (MAPK) and extracellular signal–regulated kinase–1/2 (ERK1/2) phosphorylation in rat distal pulmonary arterial smooth muscle cells (PASMCs). Cells were treated with BMP4 (50 ng/ml) for various times, from 0.25 hour up to 60 hours. (*A* and *C*) Representative Western blots indicate changes in the amount of phospho-p38 (P-p38; *A*) and phospho-ERK1/2 (P-ERK1/2; *B*) proteins in cell lysates. Cells treated with vehicle served as control samples (Cont). Total p38 (T-p38) and ERK1/2 (T-ERK1/2) proteins were also blotted to verify equal protein loading among the samples. (*B* and *D*) The intensity of P-p38 and P-ERK1/2 bands was standardized according to that of their total proteins in each sample. Values are presented as percentages of Cont. *Bars* represent means ± SEMs ($n = 5$ in each group). *$P < 0.05$, versus respective Cont.

inhibitor PD98059, followed by treatment with BMP4 (50 ng/ml) for 15 minutes. As shown in Figure 2, the inhibition of p38 by SB203580 (10 μM) completely reversed p38 activation by BMP4 (Figures 2A and 2B), but did not affect BMP4-induced ERK activation (Figures 2C and 2D). In contrast, the inhibition of ERK1/2 by PD98059 (5 μM) abolished the ERK1/2 activation induced by BMP4 (Figures 2C and 2D), without affecting p38 activation (Figures 2A and 2B). These results indicate that pretreatment with SB203580 and PD98059 is able to prevent specifically BMP4-induced activation on their target proteins p38 and ERK1/2, without detectable off-target effects.

Inhibition of p38 and ERK1/2 Prevented BMP4-Induced Increases of TRPC1, TRPC4, and TRPC6 Expression in Rat Distal PASMCs

Previously we found that BMP4 increased TRPC1, TRPC4, and TRPC6 expression in rat distal PASMCs (19). To examine whether these effects were mediated through the activation of p38 and ERK1/2, we pretreated cells with SB203580 (10 μM) or PD98059 (5 μM) for 30 minutes, followed by treatment with BMP4 (50 ng/ml) for 60 hours. As shown in Figure 3, BMP4 caused significant increases of TRPC1, TRPC4, and TRPC6 in both mRNA (Figures 3A–3C) and protein (Figures 3D–3G) concentrations, which was consistent with our previous results. However, in the presence of either SB203580 or PD98059, these increases were essentially diminished (Figure 3), suggesting that both p38 and ERK1/2 signaling are involved in the BMP4-induced up-regulation of TRPC expression in PASMCs.

Knockdown of p38 and ERK1/2 by siRNA Inhibited BMP4-Induced Increases of TRPC1, TRPC4, and TRPC6 Expression in Rat Distal PASMCs

To avoid the influence of any unknown, unspecific effects of p38 and ERK1/2 inhibitors on TRPC expression, we further used the siRNA approach to test the effects of p38 and ERK1/2 knockdown on BMP4-induced increases of TRPC expression in rat distal PASMCs. Cells were pretreated with nontargeting control (NT), p38, or ERK1/2 siRNA (50 nM) for 24 hours, followed by exposure to 50 ng/ml BMP4 for 60 hours. As shown in Figure 4A, treatment with p38 siRNA decreased p38 mRNA by more than 85%, compared with nontargeted control siRNA, without altering the mRNA expression of ERK1/2. Similar to p38 inhibition by SB203580, the knockdown of p38 by p38 siRNA caused significant decreases of TRPC1, TRPC4, and TRPC6 mRNA (Figure 4B) protein expression (Figures 4C and 4D) in the presence of BMP4.

Similarly, treatment with siRNA targeted to ERK1/2 decreased ERK1/2 mRNA in PASMCs by more than 80%, compared with NT siRNA–treated cells, without changing the mRNA expression of p38 (Figure 5A). The knockdown of ERK1/2 by ERK1/2 siRNA significantly attenuated BMP4-induced increases of TRPC1, TRPC4, and TRPC6 mRNA (Figure 5B) and protein (Figures 5C and 5D) expression in rat distal PASMCs.

Inhibition of p38 and ERK1/2 Activation and Expression Prevented BMP4-Induced Increases of Basal $[Ca^{2+}]_i$

TRPC member proteins are believed to be components of SOCCs, which can lead to enhanced SOCE, resulting in increases

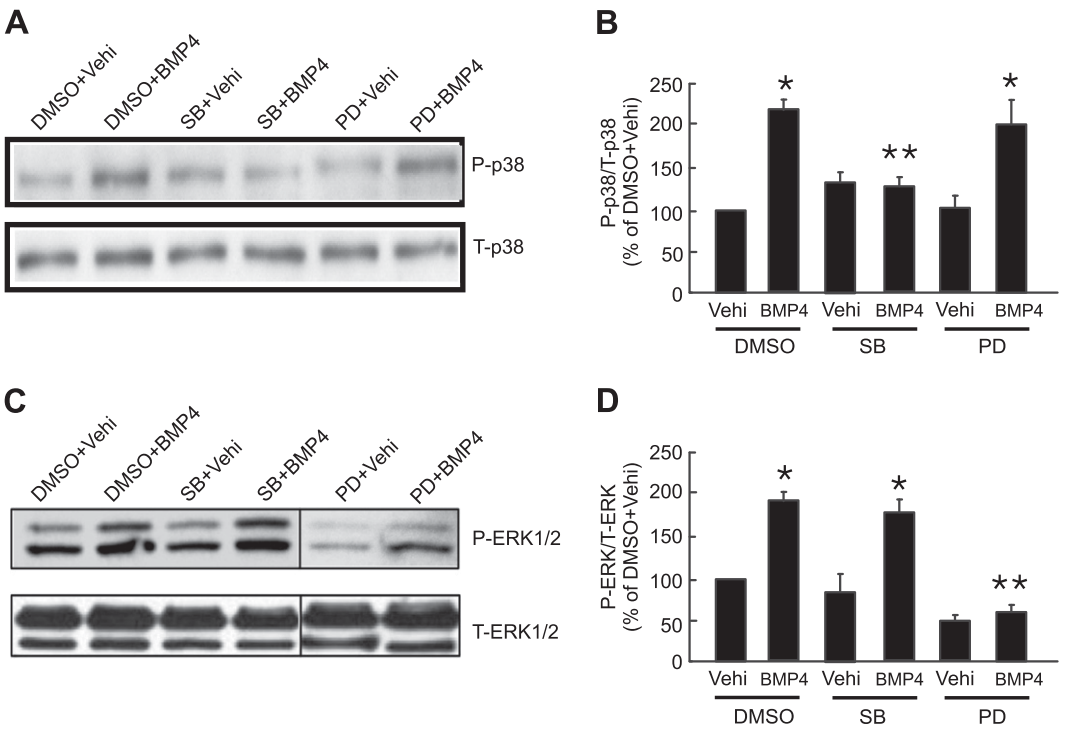

Figure 2. SB203580 (SB) and PD98059 (PD) inhibited BMP4-induced p38 and ERK1/2 phosphorylation in rat distal PASMCs. Cells were pretreated with DMSO, p38 inhibitor SB203580 (10 μM), or ERK1/2 inhibitor PD98059 (5 μM) for 30 minutes, and were then incubated with BMP4 (50 ng/ml) or its vehicle (Vehi) for 15 minutes. (*A* and *C*) Representative Western blots indicate the changes in the amount of phospho-p38 (P-p38; *A*) and phospho-ERK1/2 (P-ERK1/2; *C*) proteins in cell lysates. Total p38 (T-p38) and ERK1/2 (T-ERK1/2) proteins were also blotted to verify equal protein loading among the samples. (*B* and *D*) The intensity of the P-p38 and P-ERK1/2 bands was standardized according to that of their total proteins in each sample. Values are presented as percentages of DMSO + Vehi. *Bars* represent means ± SEMs ($n = 3$ in each group). *$P < 0.05$, compared with respective vehicle control. **$P < 0.05$, compared with DMSO + BMP4.

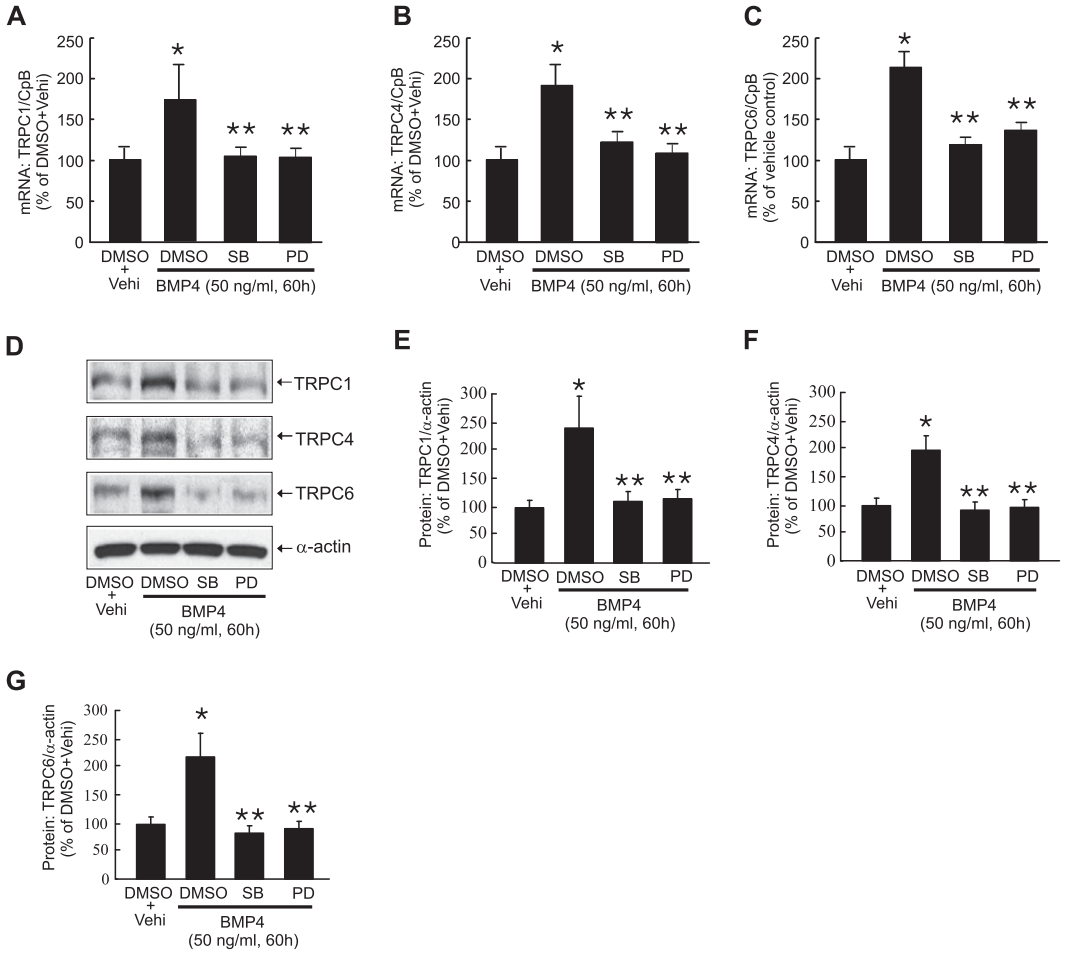

Figure 3. SB203580 and PD98059 inhibited BMP4-induced transient receptor potential (TRPC)–1, TRPC4, and TRPC6 expression in rat distal PASMCs. Cells were pretreated with DMSO, p38 inhibitor SB203580 (10 μM), or ERK1/2 inhibitor PD98059 (5 μM) for 30 minutes, and were then incubated with BMP4 (50 ng/ml) or an equal amount of BMP4 vehicle (Vehi) for 60 hours. (*A–C*) Real-time PCR demonstrated that the induction of TRPC1 (*A*), TRPC4 (*B*), and TRPC6 (*C*) mRNA in response to BMP4 was inhibited by SB203580 and PD98059. The data are presented as percentages of DMSO + Vehi. (*D*) Representative Western blots show the effects of SB203580 and PD98059 on the protein expression of TRPC1, TRPC4, and TRPC6 induced by BMP4. (*E–G*) Intensity of the TRPC1 (*E*), TRPC4 (*F*), and TRPC6 (*G*) bands was standardized by α-actin in each sample. *Bar* values indicate means ± SEMs ($n = 3$ in each group). *$P < 0.05$, compared with the respective DMSO + Vehi. **$P < 0.05$, compared with the respective DMSO + BMP4.

of basal $[Ca^{2+}]_i$ upon activation or an increase in number of SOCCs. Previous studies demonstrated that increases in TRPC expression were responsible for the increases of basal $[Ca^{2+}]_i$ in PASMCs (8). Therefore, we further observed the functional influence of the inhibition of p38 and ERK1/2 activation by their inhibitors and the knockdown of their expression on basal $[Ca^{2+}]_i$ in BMP4 (50 ng/ml)–treated PASMCs. As shown in Figure 6, pretreatment with either the p38 inhibitor (SB203580) or the ERK1/2 inhibitor (PD98059) prevented the increases in $[Ca^{2+}]_i$ caused by BMP4 (Figure 6A). The knockdown of p38 and ERK1/2 produced similar results in terms of their inhibitors (Figure 6B).

DISCUSSION

As was schematically illustrated in Figure 7, the present study provided evidence indicating that the induction of TRPC1, TRPC4, and TRPC6 expression and the elevation of basal $[Ca^{2+}]_i$ by BMP4 depends on the activation of p38 and ERK1/2 in distal PASMCs. According to the evidence gathered here, (*1*) BMP4 induced the phosphorylation of both p38 and ERK1/2 in rat distal PASMCs; (*2*) the inhibitors of either p38 or ERK1/2 activation prevented these TRPC and $[Ca^{2+}]_i$ responses to BMP4; and (*3*) the knockdown of either p38 or ERK1/2 expression also prevented the TRPC and $[Ca^{2+}]_i$ responses to BMP4.

Although both proximal and distal PAs undergo profound remodeling during the development of CHPH, their structural changes and the underlying cellular and molecular mechanisms appear to be different (20). The distal PAs are considered to be more important than the proximal PAs in the pathogenesis of CHPH, because the distal small peripheral pulmonary arteries are more susceptible to structural changes during chronic exposure to hypoxia (21–24), and they constitute the primary site of hypoxic pulmonary vasoconstriction (HPV) in the pulmonary vasculature (25). During many years of effort to elucidate the mechanisms of differential remodeling properties and differential HPV responses of proximal and distal PAs, many discrepancies between proximal and distal PASMCs have been explored, such as their proliferative responses to various growth factors (e.g., platelet-derived growth factor, angiotensin II, and transforming growth factor–β1) and hypoxia (26), the hypoxia-induced changes in $[Ca^{2+}]_i$ (27), the distribution of inositol 1,4,5-trisphosphate and ryanodine receptors in sarcoplasmic reticulum Ca^{2+} stores (28), and the expression level and function of voltage-gated potassium channels and SOCCs (17, 29). In particular, although both Smad and MAPK pathways were found to be activated to a similar extent in response to BMP4 in proximal and peripheral human PASMCs, the two types of cells seem to differ in their mechanism for the integration of these signals. As a result, proximal and peripheral human PASMCs exhibited opposing proliferative responses to BMP4: whereas the proliferation of proximal human PASMCs was inhibited, the proliferation of peripheral human PASMCs was promoted (14). Consistent with this finding, the CHPH-associated vascular wall thickening in small pulmonary vessels was greatly inhibited in mice with a partial deficiency of BMP4 (12). The mechanisms underlying these discrepant responses to BMP4 between proximal and distal PASMCs are not entirely

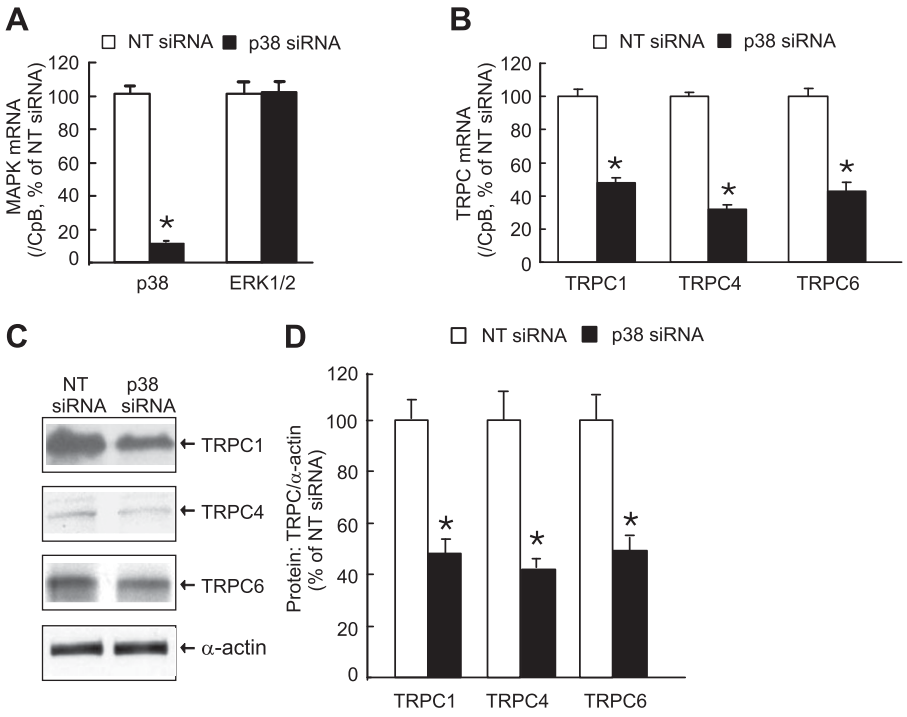

Figure 4. Effects of p38 small interfering RNA (siRNA) on BMP4-induced TRPC1, TRPC4, and TRPC6 expression in rat distal PASMCs. Cells were pretreated with p38 siRNA (50 nM) or an equal amount of nontargeting control siRNA (NT siRNA) for 24 hours, and were then incubated with BMP4 (50 ng/ml) for 60 hours. (*A*) p38 and ERK1/2 mRNA relative to cyclophilin B (CpB) was determined by real-time quantitative PCR. (*B*) TRPC1, TRPC4, and TRPC6 mRNA relative to CpB was determined by real-time quantitative PCR. (*C*) Representative Western blots of TRPC1, TRPC4, TRPC6, and α-actin protein. (*D*) *Bar graph* shows protein expression levels for TRPC1, TRPC4, and TRPC6 relative to α-actin. Data are presented as percentages of the respective NT siRNA. *Bar* values indicate means ± SEMs ($n = 3$ in each group). *$P < 0.05$, versus respective NT siRNA–treated cells.

clear, but these discrepancies may involve the differential utilization of downstream signaling by these cells, reflecting the context-specific nature of transforming growth factor (TGF)–β/BMP responses (14, 30). Therefore, instead of proximal cells, we chose distal PASMCs to start with in this study, with the long-term ultimate goal of elucidating the mechanisms behind the role of BMP4 in CHPH.

Three Type I (ALK2, BMPRIa, and BMPRIb) and three Type II (BMPRII, ActRIIa, and ActRIIb) serine–threonine kinase receptors are known to be involved in the signaling transduction of BMP4 (31). According to generally accepted knowledge, the binding of BMP4 to one of the constitutively active Type II receptors triggers the recruitment and phosphorylation of a Type I receptor. The Type I receptor subsequently causes downstream Smad-dependent and Smad-independent signaling transduction (13). In the case of Smad-dependent signaling, the activated receptor–regulated Smad proteins such as Smad1, Smad5, or Smad8 form complexes with their common

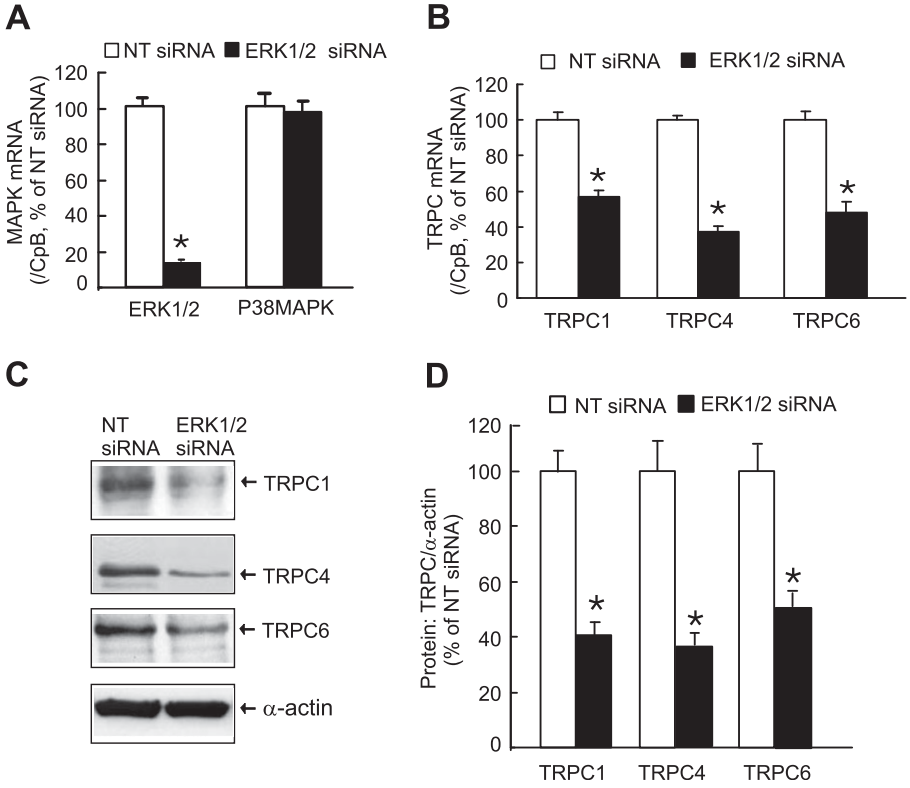

Figure 5. Effects of ERK1/2 siRNA on BMP4-induced TRPC1, TRPC4, and TRPC6 expression in rat distal PASMCs. Cells were pretreated with ERK1/2 siRNA (50 nM) or an equal amount of nontargeting control siRNA (NT siRNA) for 24 hours, and were then incubated with BMP4 (50 ng/ml) for 60 hours. (*A*) ERK1/2 and p38 mRNA relative to cyclophilin B (CpB) was determined by real-time quantitative PCR. (*B*) TRPC1, TRPC4, and TRPC6 mRNA relative to CpB was determined by real-time quantitative PCR. (*C*) Representative Western blots of TRPC1, TRPC4, TRPC6, and α-actin protein. (*D*) *Bar graph* shows protein expression levels for TRPC1, TRPC4, and TRPC6 relative to α-actin. Data are presented as percentages of the respective NT siRNA. *Bar* values indicate means ± SEMs ($n = 3$ for each group). *$P < 0.05$, versus respective NT siRNA–treated cells.

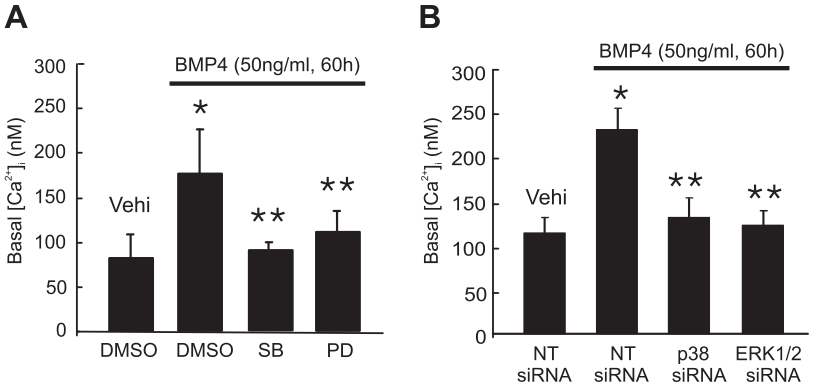

Figure 6. Inhibition of p38 and ERK1/2 activation and expression prevented BMP4-induced increases of basal intracellular Ca^{2+} ($[Ca^{2+}]_i$) in rat distal PASMCs. Cells were pretreated with DMSO, p38 inhibitor SB203580 (10 μM), or ERK1/2 inhibitor PD98059 (5 μM) for 30 minutes, or with p38, ERK1/2, or nontargeting control (NT) siRNA (50 nM) for 24 hours, and cells were then incubated with BMP4 (50 ng/ml) or an equal amount of BMP4 vehicle (Vehi) for 60 hours. (*A*) Changes in basal $[Ca^{2+}]_i$ in cells treated with DMSO + Vehi ($n = 4$ from 112 cells), DMSO + BMP4 ($n = 4$ in 135 cells), SB203580 + BMP4 ($n = 3$ from 115 cells), or PD98059 + BMP4 ($n = 3$ from 116 cells) were measured by Fura-2–based fluorescent microcopy. *Bar* values indicate means ± SEMs. *$P < 0.05$, versus Vehi control cells. **$P < 0.05$, versus Vehi + BMP4–treated cells. (*B*) Changes in basal $[Ca^{2+}]_i$ in cells treated with NT siRNA + Vehi ($n = 6$ from 177 cells), NT siRNA + BMP4 ($n = 3$ from 103 cells), p38 siRNA + BMP4 ($n = 3$ from 89 cells), and ERK1/2 siRNA + BMP4 ($n = 3$ from 97 cells). *Bar* values indicate means ± SEMs. *$P < 0.01$, versus NT siRNA + Vehi–treated cells. ** $P < 0.05$, versus NT siRNA + BMP4–treated cells.

partner Smad4 and translocate into the nucleus. In the nucleus, the Smad complex incorporates different DNA-binding cofactors that confer target gene selectivity and influence the recruitment of either transcriptional coactivators or corepressors, regulating target gene expression (32). Aside from the activation of canonical Smad signaling, increasing evidence indicates that the MAPKs, mainly ERK1/2 and p38 MAPK, were also activated by BMP4 in various cell types, including human PASMCs (12, 14, 33–35). The functional outcomes of MAPK activation by BMP4 have been linked mostly to proliferative responses, and to the regulation of various gene expressions related to cell growth and differentiation (12, 14, 36–38). Similarly, we found that BMP4 caused the activation of p38 and ERK1/2 in rat distal PASMCs, although the time-course activation patterns of p38 and ERK1/2 were different from each other, and were also somewhat different from what was documented for human peripheral PASMCs (14, 39). In the case of p38, its activation by BMP4 was obvious early on, from 15 minutes in rat PASMCs, whereas a delayed response was seen later, at 1 hour, in human cells. In both cell types, the maximum activation of ERK1/2 occurred at 0.25 hour, followed by reduced concentrations for up to 4 hours among rat PASMCs and for up to 2 hours among human cells. We do not know the mechanism responsible for these differences. Nevertheless, one aspect in common among cells of both species involves the activation of p38 by BMP4 as a sustained response, whereas the activation of ERK1/2 was transient. The molecular mechanism that leads to the differential activation patterns of p38 and ERK1/2 by BMP4 is of interest in future explorations.

Interestingly, the BMP-induced Smad-independent MAPK signaling appears to crosstalk with Smad signaling at multiple levels. For instance, in addition to activating p38, the mitogen-activated protein kinase kinase kinase 7 (TAK1) pathway has also been shown to activate ERK and Smad1/5/8 in cartilage (40). Smad signaling was thought to be inhibitory to MAPK activation. According to the evidence for this notion, in COS7 (African Green Monkey SV40-transf'd kidney fibroblast cell line) cells, phosphorylated MAPK, in cooperation with WNT/glycogen synthase kinase 3 and the Smad-specific E3 ubiquitin protein ligase–1, marks activated Smad1 for ubiquitination and proteasomal degradation (41). The overexpression of Smad1 in human embryonic kidney 293 cells reduced the phosphorylation level of TAK1, whereas the overexpression of TAK1 inhibited Smad1-mediated reporter activity. Nevertheless, the functional crosstalk among ERK, p38 MAPK, and Smad warrants future investigation.

BMPRII proved to be mandatory for BMP4-induced Smad signaling, at least in human PASMCs. The transfection of the BMPRII mutant carrying a mutation of its kinase motif disrupted Smad1 nuclear translocation without affecting p38 and ERK1/2 activation, resulting in a gain of proliferative response to BMP4 (14). Evidence from COS-1 Cell Line from African green monkey kidney suggests that the Type I receptor may be responsible for TGF-β–induced p38 activation (42). The individual roles of other BMP4 receptors in mediating differential downstream signaling and cellular function remain less well understood, and await more attention. The mechanisms linking these receptors to p38 and ERK1/2 MAPK activation are also largely unknown. The X chromosome–linked inhibitor of apoptosis protein was found to bridge the activated BMP Type I receptor to regulate TAK1-interacting protein 1 (TAB1)–TAK1 activity positively (43). TAK1 and mitogen-activated protein kinase kinase 3/6 (MKK3/6) may be responsible for BMP ligand–induced p38, and Ras family small GTPase proteins may be responsible for BMP ligand–induced ERK1/2 activation according to evidence from a number of studies (13, 43–45).

BMP4 is believed to play an important role in the pathogenesis of PAH. Yang and colleagues initially reported that BMP4 promotes the proliferation of peripheral human PASMCs (14). A subsequent milestone study by Frank and colleagues further demonstrated that BMP4 promoted PASMC proliferation and migration, resulting in the enhanced vascular remodeling of murine lungs and the development of CHPH (12). We recently found that the CH-induced up-regulation of TRPC1 and TRPC6 mediates the elevation of basal $[Ca^{2+}]_i$ through enhanced SOCE (46). Moreover, the knockdown of either TRPC1 or TRPC6 led to normalized basal $[Ca^{2+}]_i$ and the attenuated proliferation and migration of rat distal PASMCs under conditions of chronic hypoxia (8). Similar to chronic hypoxia, treatment with BMP4 alone caused the up-regulation of TRPC1, TRPC4, and TRPC6, along with increases of basal $[Ca^{2+}]_i$ in rat distal PASMCs (19). During the past two decades, since the first *TRP* was identified in *Drosophila*, much attention has been devoted to characterizing the functions of various TRP members (47). However, our understanding of TRPC regulation is limited. ERK activation has been known to up-regulate TRPC1 and TRPC6 expression (48–50). So far, no direct evidence indicates

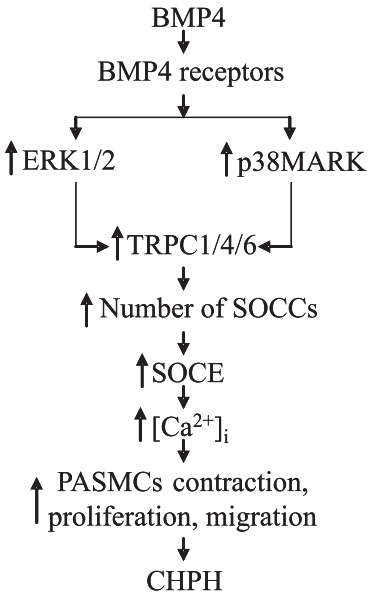

Figure 7. Schematic graph illustrates the hypothesized regulation-signaling axis of BMP4 on TRPC expression in PASMCs. BMP4 stimulation induces the activation of ERK1/2 and p38 MAPK through binding with the specific BMP receptors, which subsequently results in the up-regulation of TRPC (i.e., TRPC1, TRPC4, and TRPC6) expression. Increased TRPC concentrations could cause enhanced basal $[Ca^{2+}]_i$ through triggered store-operated calcium entry (SOCE), eventually leading to PASMC contraction, proliferation, and migration, which relates to the pathogenesis of chronic hypoxic pulmonary hypertension (CHPH). SOCCs, store-operated calcium channels.

how p38 activation leads to the up-regulation of TRPC expression. This study further determined that the involvement of p38 and ERK1/2 activation in BMP4 induced TRPC expression and increases of basal $[Ca^{2+}]_i$ in PASMCs. We first selected and used the well-recognized chemical inhibitors SB203580 for p38 MAPK and PD98059 for ERK1/2, to block individual pathways. Treatment with SB203580 or PD98059 resulted in a specific diminution of either p38MAPK or ERK1/2 activation, respectively, without cross-activation, confirming their efficiency and specificity. Moreover, we used the siRNA approach to knock down p38 and ERK1/2 expression individually, and then assessed their effects on BMP4-induced TRPC and basal $[Ca^{2+}]_i$ responses. Previous studies with serial doses of BMP4 and various treatment times (24–60 hours) demonstrated that BMP4 up-regulated TRPC1, TRPC4, and TRPC6 expression, with the maximum induction of TRPC expression observed at 50 ng/ml for 60 hours. This induction of TRPC expression was associated with an elevation of basal $[Ca^{2+}]_i$ in rat distal PASMCs (19). In the present study, this treatment condition for maximal responses to BMP4 was also used for all TRPC and basal $[Ca^{2+}]_i$ measurements. As a result, we found that both ERK1/2 and p38 are required for BMP4-induced TRPC1, TRPC4, and TRPC6 expression and basal $[Ca^{2+}]_i$ induction to BMP4 in distal PASMCs. The inhibition or knockdown of either ERK1/2 or p38 substantially abolished these responses.

The substrate spectrum of activated MAPKs is extremely wide, consisting not only of their downstream kinases, but also of various transcription factors, membrane proteins, and cytoskeleton proteins (51). Given that members of the MAPK family often share overlapping specificities for their substrates, it is reasonable to assume that p38 and ERK may share both common and distinguished mechanisms in their regulation of TRPC (51). The fact that both are required for BMP4-induced TRPC expression suggests essential downstream crosstalk between them in the signaling to effect TRPC regulation.

In conclusion, this study provides mechanistic insights into the function of BMP4 in regulating Ca^{2+} homeostasis in distal PASMCs, indicating that a signaling cascade of BMP4–p38/ERK–TRPC–basal $[Ca^{2+}]_i$ is involved. This cascade could be basically defined in terms of BMP4 binding with its specific receptors, thus inducing the activation of ERK1/2, subsequently resulting in the up-regulation of TRPC (i.e., TRPC1, TRPC4, and TRPC6) expression. This up-regulated TRPC expression could cause increased numbers of SOCCs, contributing to enhanced basal $[Ca^{2+}]_i$ through triggered SOCEs, eventually leading to the contraction, proliferation, and migration of PASMCs, which relates to the pathogenesis of CHPH. Given that basal $[Ca^{2+}]_i$ is crucial for both the constriction and proliferation of vascular smooth muscle cells, this signaling likely contributes to decipher the pathogenetic role of BMP4 in promoting pulmonary vascular remodeling and the development of pulmonary hypertension. A future study is warranted, directed toward examining whether this signaling discovered in cells *in vitro* can be translated into cells *in vivo*.

Author disclosures are available with the text of this article at www.atsjournals.org.

References

1. Wang J, Weigand L, Lu W, Sylvester JT, Semenza GL, Shimoda LA. Hypoxia inducible factor 1 mediates hypoxia-induced TRPC expression and elevated intracellular Ca^{2+} in pulmonary arterial smooth muscle cells. *Circ Res* 2006;98:1528–1537.
2. Lin MJ, Leung GP, Zhang WM, Yang XR, Yip KP, Tse CM, Sham JS. Chronic hypoxia-induced upregulation of store-operated and receptor-operated Ca^{2+} channels in pulmonary arterial smooth muscle cells: a novel mechanism of hypoxic pulmonary hypertension. *Circ Res* 2004;95:496–505.
3. Shimoda LA, Wang J, Sylvester JT. Ca^{2+} channels and chronic hypoxia. *Microcirculation* 2006;13:657–670.
4. Karaki H, Ozaki H, Hori M, Mitsui-Saito M, Amano K, Harada K, Miyamoto S, Nakazawa H, Won KJ, Sato K. Calcium movements, distribution, and functions in smooth muscle. *Pharmacol Rev* 1997; 49:157–230.
5. Shimoda LA, Sham JS, Shimoda TH, Sylvester JT. L-type Ca^{2+} channels, resting $[Ca^{2+}]_i$, and ET-1–induced responses in chronically hypoxic pulmonary myocytes. *Am J Physiol Lung Cell Mol Physiol* 2000;279: L884–L894.
6. Remillard CV, Yuan JX. TRP channels, CCE, and the pulmonary vascular smooth muscle. *Microcirculation* 2006;13:671–692.
7. Wang J, Shimoda LA, Sylvester JT. Capacitative calcium entry and TRPC channel proteins are expressed in rat distal pulmonary arterial smooth muscle. *Am J Physiol Lung Cell Mol Physiol* 2004; 286:L848–L858.
8. Lu W, Ran P, Zhang D, Peng G, Li B, Zhong N, Wang J. Sildenafil inhibits chronically hypoxic upregulation of canonical transient receptor potential expression in rat pulmonary arterial smooth muscle. *Am J Physiol Cell Physiol* 2010;298:C114–C123.
9. Rider CC, Mulloy B. Bone morphogenetic protein and growth differentiation factor cytokine families and their protein antagonists. *Biochem J* 2010;429: 1–12.
10. Weaver M, Yingling JM, Dunn NR, Bellusci S, Hogan BL. BMP signaling regulates proximal–distal differentiation of endoderm in mouse lung development. *Development* 1999;126:4005–4015.
11. Weaver M, Dunn NR, Hogan BL. BMP4 and FGF10 play opposing roles during lung bud morphogenesis. *Development* 2000;127:2695–2704.
12. Frank DB, Abtahi A, Yamaguchi DJ, Manning S, Shyr Y, Pozzi A, Baldwin HS, Johnson JE, de Caestecker MP. Bone morphogenetic protein 4 promotes pulmonary vascular remodeling in hypoxic pulmonary hypertension. *Circ Res* 2005;97:496–504.
13. Derynck R, Zhang YE. Smad-dependent and Smad-independent pathways in TGF-beta family signalling. *Nature* 2003;425:577–584.
14. Yang X, Long L, Southwood M, Rudarakanchana N, Upton PD, Jeffery TK, Atkinson C, Chen H, Trembath RC, Morrell NW. Dysfunctional Smad signaling contributes to abnormal smooth muscle cell proliferation in familial pulmonary arterial hypertension. *Circ Res* 2005;96:1053–1063.
15. Morty RE, Nejman B, Kwapiszewska G, Hecker M, Zakrzewicz A, Kouri FM, Peters DM, Dumitrascu R, Seeger W, Knaus P, *et al.* Dysregulated bone morphogenetic protein signaling in monocrotaline-induced pulmonary arterial hypertension. *Arterioscler Thromb Vasc Biol* 2007;27: 1072–1078.
16. Yu PB, Deng DY, Beppu H, Hong CC, Lai C, Hoyng SA, Kawai N, Bloch KD. Bone morphogenetic protein (BMP) Type II receptor is required for BMP-mediated growth arrest and differentiation in pulmonary artery smooth muscle cells. *J Biol Chem* 2008;283:3877–3888.

17. Lu W, Wang J, Shimoda LA, Sylvester JT. Differences in STIM1 and TRPC expression in proximal and distal pulmonary arterial smooth muscle are associated with differences in Ca^{2+} responses to hypoxia. *Am J Physiol Lung Cell Mol Physiol* 2008;295:L104–L113.
18. Pfaffl MW. A new mathematical model for relative quantification in real-time RT-PCR. *Nucleic Acids Res* 2001;29:e45.
19. Lu W, Ran P, Zhang D, Lai N, Zhong N, Wang J. Bone morphogenetic protein 4 enhances canonical transient receptor potential expression, store-operated Ca^{2+} entry, and basal $[Ca^{2+}]_i$ in rat distal pulmonary arterial smooth muscle cells. *Am J Physiol Cell Physiol* 2010;299:C1370–C1378.
20. Stenmark KR, Fagan KA, Frid MG. Hypoxia-induced pulmonary vascular remodeling: cellular and molecular mechanisms. *Circ Res* 2006; 99:675–691.
21. Abraham AS, Kay JM, Cole RB, Pincock AC. Haemodynamic and pathological study of the effect of chronic hypoxia and subsequent recovery of the heart and pulmonary vasculature of the rat. *Cardiovasc Res* 1971;5:95–102.
22. Hislop A, Reid L. Changes in the pulmonary arteries of the rat during recovery from hypoxia-induced pulmonary hypertension. *Br J Exp Pathol* 1977;58:653–662.
23. Meyrick B, Reid L. The effect of chronic hypoxia on pulmonary arteries in young rats. *Exp Lung Res* 1981;2:257–271.
24. Rabinovitch M, Gamble W, Nadas AS, Miettinen OS, Reid L. Rat pulmonary circulation after chronic hypoxia: hemodynamic and structural features. *Am J Physiol* 1979;236:H818–H827.
25. Schwenke DO, Pearson JT, Umetani K, Kangawa K, Shirai M. Imaging of the pulmonary circulation in the closed-chest rat using synchrotron radiation microangiography. *J Appl Physiol* 2007;102:787–793.
26. Stiebellehner L, Frid MG, Reeves JT, Low RB, Gnanasekharan M, Stenmark KR. Bovine distal pulmonary arterial media is composed of a uniform population of well-differentiated smooth muscle cells with low proliferative capabilities. *Am J Physiol Lung Cell Mol Physiol* 2003;285:L819–L828.
27. Bakhramov A, Evans AM, Kozlowski RZ. Differential effects of hypoxia on the intracellular Ca^{2+} concentration of myocytes isolated from different regions of the rat pulmonary arterial tree. *Exp Physiol* 1998; 83:337–347.
28. Urena J, Smani T, Lopez-Barneo J. Differential functional properties of Ca^{2+} stores in pulmonary arterial conduit and resistance myocytes. *Cell Calcium* 2004;36:525–534.
29. Archer SL, Wu XC, Thebaud B, Nsair A, Bonnet S, Tyrrell B, McMurtry MS, Hashimoto K, Harry G, Michelakis ED. Preferential expression and function of voltage-gated, O_2-sensitive K^+ channels in resistance pulmonary arteries explains regional heterogeneity in hypoxic pulmonary vasoconstriction: ionic diversity in smooth muscle cells. *Circ Res* 2004;95:308–318.
30. Schulick AH, Taylor AJ, Zuo W, Qiu CB, Dong G, Woodward RN, Agah R, Roberts AB, Virmani R, Dichek DA. Overexpression of transforming growth factor beta1 in arterial endothelium causes hyperplasia, apoptosis, and cartilaginous metaplasia. *Proc Natl Acad Sci USA* 1998;95:6983–6988.
31. de Caestecker M. The transforming growth factor–beta superfamily of receptors. *Cytokine Growth Factor Rev* 2004;15:1–11.
32. Massague J, Seoane J, Wotton D. Smad transcription factors. *Genes Dev* 2005;19:2783–2810.
33. Nohe A, Keating E, Knaus P, Petersen NO. Signal transduction of bone morphogenetic protein receptors. *Cell Signal* 2004;16:291–299.
34. Zhou Q, Heinke J, Vargas A, Winnik S, Krauss T, Bode C, Patterson C, Moser M. ERK signaling is a central regulator for BMP-4 dependent capillary sprouting. *Cardiovasc Res* 2007;76:390–399.
35. Moon BS, Yoon JY, Kim MY, Lee SH, Choi T, Choi KY. Bone morphogenetic protein 4 stimulates neuronal differentiation of neuronal stem cells through the ERK pathway. *Exp Mol Med* 2009;41:116–125.
36. Jeffery TK, Upton PD, Trembath RC, Morrell NW. BMP4 inhibits proliferation and promotes myocyte differentiation of lung fibroblasts via Smad1 and JNK pathways. *Am J Physiol Lung Cell Mol Physiol* 2005;288:L370–L378.
37. Dewachter L, Adnot S, Guignabert C, Tu L, Marcos E, Fadel E, Humbert M, Dartevelle P, Simonneau G, Naeije R, *et al.* Bone morphogenetic protein signalling in heritable versus idiopathic pulmonary hypertension. *Eur Respir J* 2009;34:1100–1110.
38. Lee JS, Ha L, Park JH, Lim JY. Mechanical stretch suppresses BMP4 induction of stem cell adipogenesis via upregulating ERK but not through downregulating Smad or p38. *Biochem Biophys Res Commun* 2012;418:278–283.
39. Yang X, Lee PJ, Long L, Trembath RC, Morrell NW. BMP4 induces HO-1 via a Smad-independent, p38MAPK-dependent pathway in pulmonary artery myocytes. *Am J Respir Cell Mol Biol* 2007;37:598–605.
40. Shim JH, Greenblatt MB, Xie M, Schneider MD, Zou W, Zhai B, Gygi S, Glimcher LH. TAK1 is an essential regulator of BMP signalling in cartilage. *EMBO J* 2009;28:2028–2041.
41. Fuentealba LC, Eivers E, Ikeda A, Hurtado C, Kuroda H, Pera EM, De Robertis EM. Integrating patterning signals: WNT/GSK3 regulates the duration of the BMP/Smad1 signal. *Cell* 2007;131:980–993.
42. Yu L, Hebert MC, Zhang YE. TGF-beta receptor–activated p38 MAP kinase mediates Smad-independent TGF-beta responses. *EMBO J* 2002;21:3749–3759.
43. Yamaguchi K, Nagai S, Ninomiya-Tsuji J, Nishita M, Tamai K, Irie K, Ueno N, Nishida E, Shibuya H, Matsumoto K. XIAP, a cellular member of the inhibitor of apoptosis protein family, links the receptors to TAB1–TAK1 in the BMP signaling pathway. *EMBO J* 1999;18:179–187.
44. Yue J, Mulder KM. Activation of the mitogen-activated protein kinase pathway by transforming growth factor–beta. *Methods Mol Biol* 2000; 142:125–131.
45. Hartsough MT, Frey RS, Zipfel PA, Buard A, Cook SJ, McCormick F, Mulder KM. Altered transforming growth factor signaling in epithelial cells when Ras activation is blocked. *J Biol Chem* 1996;271:22368–22375.
46. Wang J, Semenza G, Sylvester JT, Shimoda LA. HIF-1 regulates hypoxic-induction of canonical transient receptor potential (TRPC) channels in pulmonary arterial smooth muscle cells [abstract]. *FASEB J* 2005;19:A1278.
47. Montell C, Rubin GM. Molecular characterization of the *Drosophila* TRP locus: a putative integral membrane protein required for phototransduction. *Neuron* 1989;2:1313–1323.
48. El Hiani Y, Lehen'kyi V, Ouadid-Ahidouch H, Ahidouch A. Activation of the calcium-sensing receptor by high calcium induced breast cancer cell proliferation and TRPC1 cation channel over-expression potentially through EGFR pathways. *Arch Biochem Biophys* 2009;486:58–63.
49. Zhang H, Ding J, Fan Q, Liu S. TRPC6 up-regulation in Ang II–induced podocyte apoptosis might result from ERK activation and NF-kappaB translocation. *Exp Biol Med (Maywood)* 2009; 234:1029–1036.
50. Paria BC, Malik AB, Kwiatek AM, Rahman A, May MJ, Ghosh S, Tiruppathi C. Tumor necrosis factor–alpha induces nuclear factor–kappaB–dependent TRPC1 expression in endothelial cells. *J Biol Chem* 2003;278:37195–37203.
51. Pearson G, Robinson F, Beers Gibson T, Xu BE, Karandikar M, Berman K, Cobb MH. Mitogen-activated protein (MAP) kinase pathways: regulation and physiological functions. *Endocr Rev* 2001;22:153–183.